

NACA TN 3666

3966

NATIONAL ADVISORY COMMITTEE FOR AERONAUTICS

TECHNICAL NOTE 3666

BODIES OF REVOLUTION HAVING MINIMUM DRAG AT HIGH SUPERSONIC AIRSPEEDS

By A. J. Eggers, Jr., Meyer M. Resnikoff,
and David H. Dennis

Ames Aeronautical Laboratory
Moffett Field, Calif.



Washington
February 1956

AFMDC
TECHNICAL NOTE 3666





TECHNICAL NOTE 3666

BODIES OF REVOLUTION HAVING MINIMUM DRAG

AT HIGH SUPERSONIC AIRSPEEDS¹

By A. J. Eggers, Jr., Meyer M. Resnikoff,
and David H. Dennis

SUMMARY

Approximate shapes of nonlifting bodies having minimum pressure fore-drag at high supersonic airspeeds are calculated. With the aid of Newton's law of resistance, the investigation is carried out for various combinations of the conditions of given body length, base diameter, surface area, and volume. In general, it is found that when body length is fixed, the body has a blunt nose; whereas, when the length is not fixed, the body has a sharp nose. The additional effect of curvature of the flow over the surface is investigated to determine its influence on the shapes for minimum drag. The effect is to increase the bluntness of the shapes in the region of the nose and the curvature in the region downstream of the nose. These shape modifications have, according to calculation, only a slight tendency to reduce drag.

Several bodies of revolution of fineness ratios 3 and 5, including the calculated shapes of minimum drag for given length and base diameter and for given base diameter and surface area, were tested at Mach numbers from 2.73 to 6.28. A comparison of theoretical and experimental foredrag coefficients indicates that the calculated minimum-drag bodies are reasonable approximations to the correct shapes. It is verified, for example, that the body for a given length and base diameter has as much as 20 percent less foredrag than a cone of the same fineness ratio.

INTRODUCTION

The shapes of nonlifting bodies of revolution having minimum pressure drag at supersonic speeds have been the subject of numerous theoretical investigations. Kármán (reference 1) determined the shape of such a body (neglecting base drag) with given length and base diameter. Somewhat

¹Supersedes NACA RM A51K27, "Bodies of Revolution for Minimum Drag at High Supersonic Airspeeds," by A. J. Eggers, Jr., David H. Dennis, and Meyer M. Resnikoff, 1952, and NACA RM A52D24, "Supplementary Note on Modified-Impact-Theory Calculations for Bodies of Revolution Having Minimum Drag at Hypersonic Speeds," by Meyer M. Resnikoff, 1952.

later Haack (reference 2), Ferrari (reference 3), Lighthill (reference 4), and Sears (reference 5) calculated body shapes having minimum pressure drag for various other given conditions using methods similar to those first employed by Kármán. In all these investigations the assumption of small perturbation, potential flow was made. It is to be expected, therefore, that the shapes obtained by these investigators are representative of minimum-drag body shapes of practical fineness ratios at low supersonic Mach numbers.

Perhaps the first calculation of the shape of a body having minimum drag was made by Newton (reference 6) using a method analogous to the present day calculus of variations. Newton was concerned with determining the body of given length and base diameter having minimum resistance when moving at sufficiently high speeds to insure that the inertia forces are large compared to the elastic forces in the immersing fluid. Thus, as shown by Sanger (reference 7) and Epstein (reference 8), the law of resistance adopted by Newton approximates that (neglecting viscous forces) for hypersonic air flows. According to this law, the local resisting pressure is proportional to the square of the free-stream velocity component normal to the body surface. Legendre (see, e.g., reference 9) further investigated Newton's problem and concluded that if no restrictions were imposed on the variation of slope along the surface, a body having a meridian curve composed of jagged lines (sharp edges forward) could be constructed which, with this law of resistance, would have less drag than Newton's body. It may easily be deduced, however, that Newton's law of resistance would not be satisfied on the surface of Legendre's body since gas would be trapped in a number of regions along the jagged contour. It may be shown in fact that when this law of resistance is satisfied at the surface - in which case the surface angles must lie between 0 and $\pi/2$ radians - then Newton's body may be considered the minimum pressure drag body for the given conditions.

It has been undertaken in the present report, using Newton's law of resistance and the calculus of variations, to determine body shapes having minimum pressure drag (neglecting base drag) at high supersonic speeds for various combinations of the conditions of given length, base diameter, surface area, and volume. The effect of curvature of the flow over the surface is also investigated to determine its influence on the shapes for minimum drag.

Several bodies of revolution, including two of the bodies determined from this analysis, were tested at Mach numbers from 2.73 to 6.28 in the Ames 10- by 14-inch supersonic wind tunnel. Foredrag data at zero lift obtained from these tests are compared with the analytic predictions to assess the accuracy of the theoretical considerations.

SYMBOLS

- A local cross-sectional area of body
- a local speed of sound
- C_D drag coefficient $\left(\frac{4D}{q_0 \pi d^2} \right)$
- C_p pressure coefficient $\left(\frac{p - p_0}{q_0} \right)$
- c constant of integration
- D pressure foredrag
- d maximum body diameter
- f integrand function
- I_D drag parameter $\left(\frac{D}{2\pi q_0} \right)$
- K hypersonic similarity parameter $\left(M_0 \frac{d}{l} \right)$
- l body length
- M Mach number $\left(\frac{U}{a} \right)$
- N distance measured normal to surface of body
- n exponent in equation defining shapes of experimental test bodies
- p static pressure
- q dynamic pressure
- R radius of curvature of streamline in plane containing axis of symmetry (i.e., meridian plane) of body
- S body surface area
- U resultant velocity
- V body volume
- x,y coordinates of point on meridian curve of body (origin of coordinate system coincides with nose of body, and X axis coincides with axis of symmetry)

- γ ratio of specific heat at constant pressure to specific heat at constant volume
- δ angle (in meridian plane) between free-stream direction and tangent to body surface
- λ Lagrange multiplier
- ρ density

Subscripts

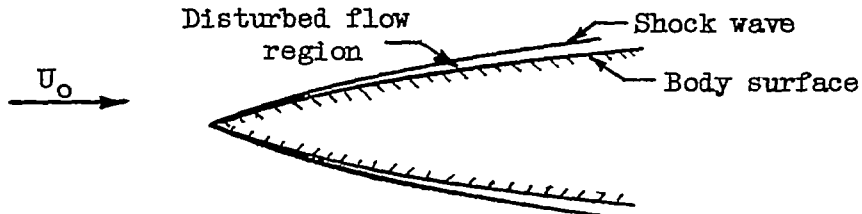
- $_{\infty}$ free-stream conditions
- $_1$ values at nose point of meridian curve
- $_2$ values at base point of minimizing curve
- $+$ right-hand limiting value of quantity at corner on minimizing curve
- $-$ left-hand limiting value of quantity at corner on minimizing curve
- B values along meridian curve
- c cone values

THEORY

The investigation undertaken here is concerned with the shapes of nonlifting bodies of revolution having minimum pressure foredrag at high supersonic airspeeds. Difficulties inherent in the calculation of these shapes make it desirable to simplify the drag equation insofar as is practicable, consistent with retaining the salient features of the dependence of drag on body shape and free-stream conditions. Likewise, in view of the several conditions to be treated (viz., given length, base diameter, volume, and surface area), it is convenient to set up a procedure of analysis to fit the general problem at hand. These fundamental considerations will be discussed prior to the determination of specific minimum-drag shapes.

Fundamental Considerations

Simplified drag theory.— As pointed out in the introduction, Newton's law of resistance applies approximately to bodies traveling at high supersonic airspeeds. This observation has basis in the fact that at such speeds the inertia forces predominate over the elastic forces in the disturbed air. Thus, oblique shock flows approach the corpuscular-type flows treated by Newton as the Mach number of the free stream becomes large compared to 1. If it is further assumed that γ of the disturbed fluid approaches 1,² the shock-wave angle approaches the flow-deflection angle (see sketch). In this case the pressure



coefficient at a point just downstream of the wave is given by the simple expression (reference 8).

$$C_p = 2 \sin^2 \delta \quad (1)$$

This equation is recognized, of course, as being (aside from the constant multiplier) a mathematical statement of Newton's law of resistance for corpuscular or impact-type flow.

When the curvature of the body, and hence of the disturbed flow, is small in the stream direction, equation (1) should also predict the pressure coefficients at the surface of a body since, in this case, the centrifugal forces in the thin layer of air (sometimes referred to as the hypersonic boundary layer) between the shock and the surface should not appreciably alter the impact pressures. When the curvature of the body is large in the stream direction, centrifugal forces in the fluid between the shock and the surface may alter the pressures at the surface

²This assumption was perhaps first suggested by Epstein (reference 8). It has the advantage of simplifying the impact force analysis without significantly influencing its accuracy. In other words, these forces in flows about axially symmetric bodies are relatively insensitive to changes in γ from 1.4 to 1. Interestingly enough, present indications are that disturbed air flows in flight at extremely high Mach numbers will be characterized by values of γ below 1.4 (see references 10 and 11).

from those just downstream of the shock. Busemann (reference 12) investigated this problem and found that the pressure coefficient at a point on the surface of a body curved in the stream direction is given by the relation

$$C_p = 2 \left(\sin^2 \delta + \sin \delta \frac{d\delta}{dA} \int_0^A \cos \delta dA \right) \quad (2)$$

in the limit as $M \rightarrow \infty$ and $\gamma \rightarrow 1$.

In order to assess the accuracy with which the preceding equations may be expected to provide the pressure distributions, and thus pressure drags, on bodies operating at high supersonic airspeeds, the predictions of these equations are compared in figure 1 with those of the method of characteristics (obtained from reference 13) for an ogive operating at a value of the hypersonic similarity parameter K (ratio of free-stream Mach number to slenderness ratio) equal to 2, corresponding to a free-stream Mach number of 6. It is evident that the theory of Busemann (equation (2)) yields far too low pressures downstream of the nose, while the simple impact theory (equation (1)) is in reasonably good over-all agreement with the method of characteristics.³ The relatively poor predictions of the Busemann theory are associated with the fact that it strongly overestimates centrifugal-force effects at free-stream Mach numbers which are large compared to 1, but for which γ of the air flow downstream of the bow shock is closer to 1.4 than 1 (i.e., at flow conditions of principal interest in this paper). This matter will be discussed in greater detail later in the paper. Agreement comparable to that just discussed is obtained with the other results presented in reference 13 for $K = 2$. For lower values of K the agreement of the impact theory with the method of characteristics is somewhat poorer, as would be expected; however, it does not become unacceptably poor except for values of K below 1 (e.g., the pressure coefficients differ by from 0 to 35 percent for a K of 1/2). It is therefore concluded that for values of K greater than 1, equation (1) may be used with acceptable accuracy for the purposes of this paper to predict the pressure distributions and thus pressure drags on bodies.⁴

³The characteristics solutions of reference 13 were carried out for $\gamma = 1.4$. Free flight at the larger values of K considered in this report would produce values of γ downstream of the bow shock slightly less than 1.4; however, the small decreases in γ would not significantly alter the results presented.

⁴The approximate theory of reference 14 might also be employed in an analysis of this type - this theory is, in fact, more accurate than those discussed, so long as the flow is everywhere supersonic. However, the theories considered here have the advantage, as will be apparent later, of predicting approximately correct values of surface pressures for arbitrarily large surface slopes.

For this reason, and because of its simplicity, it is employed throughout the subsequent analysis.

If the manner in which the pressure coefficient varies over the surface is known, it is a simple matter, of course, to evaluate the pressure drag of a body. Neglecting the base-drag contribution, we have then

$$D = \frac{C_D q_0 \pi d^2}{4} = 2\pi q_0 \int_0^l C_p y y' dx \quad (3)$$

where y' denotes the derivative dy/dx . This equation may be expressed in a form more convenient for use here

$$I_D = \frac{D}{2\pi q_0} = \int_0^l C_p y y' dx \quad (4)$$

If C_p in this expression is replaced by its value given in equation (1) (noting that $\sin^2 \delta = \frac{y'^2}{1+y'^2}$), there is then obtained the relation

$$I_D = \int_0^l \frac{2yy'^3}{1+y'^2} dx \quad (5)$$

It remains now to consider the procedure for employing this expression in combination with the methods of the variational calculus in order to determine the desired minimum-drag body shapes.

Procedure for Calculating Minimum-Drag Bodies

The calculation of minimum-drag body shapes of interest here is equivalent to determining the form of the function $y = y(x)$ which minimizes the integral defined in equation (5) for the various given conditions. In considering the procedure for carrying out this calculation, however, it is convenient, for reasons that will be apparent later, to write equation (5) in a form which effectively yields the total drag as the sum of the drag on any finite region of infinite slope at the nose plus the drag on the surface downstream of the nose. Thus we have

$$I_D = y_1^2 + \int_0^{x_2} \frac{2yy'^3}{1+y'^2} dx \quad (6)$$

where the variable limit x_2 is introduced to permit variations in body length. The conditions of given volume or given surface area are fixed by the auxiliary requirements that, respectively,

$$\frac{V}{\pi} = \int_0^{x_2} y^2 dx = \text{const.} \quad (7)$$

or (neglecting base area)

$$\frac{S}{2\pi} = \frac{y_1^2}{2} + \int_0^{x_2} y \sqrt{1+y'^2} dx = \text{const.} \quad (8)$$

When the length and base diameter are given, the problem is simply to minimize the function I_D given by equation (6). However, according to the isoperimetric rule of the calculus of variations (see, e.g., reference 15), the problem of minimizing the function I_D , subject to the auxiliary condition given by equation (7) or (8), is equivalent to minimizing the new function J_D , where

$$J_D = I_D + \lambda \frac{V}{\pi} \quad (9)$$

or

$$J_D = I_D + \lambda \frac{S}{2\pi} \quad (10)$$

depending on whether the volume or surface area is given. The parameter λ is a constant, sometimes called the Lagrange multiplier.

With the aid of equations (6) through (10), the integrand functions to be minimized can be immediately written. These functions are as follows:

case a, given length and base diameter

$$f = \frac{2yy'^3}{1+y'^2} \quad (11)$$

case b, given volume and length or base diameter

$$f = \frac{2yy'^3}{1+y'^2} + \lambda y^2 \quad (12)$$

case c, given surface area and length or base diameter

$$f = \frac{2yy'^3}{1+y'^2} + \lambda y \sqrt{1+y'^2} \quad (13)$$

Now any function $y = y(x)$ which minimizes equation (6), (9), or (10) must, irrespective of the given conditions, satisfy the Euler equation (for zero first variation of I_D or J_D with small changes in the function $y(x)$)

$$\frac{d}{dx} f_{y'} - f_y = 0 \quad (14)$$

where $f_{y'}$ and f_y denote the partial derivatives $\frac{\partial f}{\partial y'}$ and $\frac{\partial f}{\partial y}$, respectively. Since the integrand functions given above are free of the independent variable, the first integral of the Euler equation for these functions follows immediately, namely,

$$y' f_{y'} - f = \text{const.} \quad (15)$$

Substituting, successively, equations (11), (12), and (13) into this equation there are then obtained the expressions

$$\frac{4yy'^3}{(1+y'^2)^2} = \text{const.} \quad (16)$$

$$\frac{4yy'^3}{(1+y'^2)^2} - \lambda y^2 = \text{const.} \quad (17)$$

and

$$y \left[\frac{4y'^3}{(1+y'^2)^2} - \frac{\lambda}{\sqrt{1+y'^2}} \right] = \text{const.} \quad (18)$$

for cases a, b, and c, respectively. Solutions to these differential equations satisfying the terminal conditions on the bodies are minimizing curves for the given conditions.

When the end points of a minimizing curve are not fixed, other terminal conditions must be imposed on the function $y = y(x)$. Thus, to determine the ordinate at the nose, it is required that (see reference 16)

$$\left(f_{y'} - \frac{d}{dy} y^2 \right) \Big|_{y=y_1} = 2y \frac{y'^2 - 1}{(1+y'^2)^2} \Big|_{y=y_1} = 0 \quad (19)$$

for cases a and b, while

$$\left[f_{y'} - \frac{d}{dy} \left(y^2 + \lambda \frac{y'^2}{2} \right) \right]_{y=y_1} = y_1 \left[2 \frac{y'^4 + 3y'^2}{(1+y'^2)^2} + \sqrt{\frac{\lambda y'^2}{1+y'^2}} - (2+\lambda) \right]_{y=y_1} = 0 \quad (20)$$

for case c. Similarly, when the length is not given it is necessary that

$$\left(y' f_{y'} - f \right) \Big|_{x=x_2} = 0 \quad (21)$$

and when the base diameter is not given it is required that

$$f_{y'} \Big|_{x=x_2} = 0 \quad (22)$$

In addition to the above described conditions, two checks must be made to determine completely the shape of a minimizing curve. The first of these checks entails ascertaining whether there are any corners (between the end points) on the curve. This is accomplished by determining whether the function $y = y(x)$ can satisfy the requirement that (see reference 15)

$$f_{y'+} = f_{y'-} \quad (23)$$

at a point of discontinuity in y' . If this equation is not satisfied, no corners exist. The second check requires that the Legendre condition (for a positive second variation),

$$f_{y'y'} \geq 0 \quad (24)$$

be satisfied everywhere on the curve. With the aid of these checks, the minimizing curves for various combinations of the conditions of given length, base diameter, volume, and surface area can be uniquely defined. The calculation of these curves for several such combinations is now undertaken.

Calculation of Minimum-Drag Bodies

Given length and base diameter.— Equations (16) and (19) give the first integral to Euler's equation and the terminal condition at the nose, respectively, for these given conditions. It is evident upon examining these equations that the minimizing curve cannot, in general, pass through both the points $(0,0)$ and (x_2, y_2) , but must, in fact, have its forward termination point at $(0, y_1)$ with $y_1' = 1$. With this information, the minimizing curve can be represented in parametric form, namely,

$$\left. \begin{aligned} y &= \frac{y_1}{4} \frac{(1+y'^2)^2}{y'} \\ x &= \frac{y_1}{4} \left(\frac{3}{4y'^4} + \frac{1}{y'^2} - \frac{7}{4} + \ln y' \right) \end{aligned} \right\} \quad (25)$$

It is easily shown with the solution to the Euler equation and equation (23) that there are no corners on the minimizing curve;⁵ thus the variation of y with x is readily determined with the relations of equation (25) for a given λ and d (corresponding to a given x_2 and y_2) of a body. These relations for a body of given fineness ratio can be shown to be equivalent to those originally developed by Newton (see reference 6).

Given length and volume.— For these given conditions, the terminal conditions (equations (19) and (22)) require the slopes at the nose and at the base to be, respectively, $y_1' = 1$ and $y_2' = 0$. The first integral to the Euler expression (equation (17)) then leads to the following parametric representation of the minimizing curve:

$$\left. \begin{aligned} y &= \frac{2y'^3}{\lambda(1+y'^2)^2} + \sqrt{\left[\frac{2y'^3}{\lambda(1+y'^2)^2} \right]^2 - \frac{y_1 - \lambda y_1^2}{\lambda}} \\ x &= \int_{y_1}^y \frac{dy}{y'} \end{aligned} \right\} \quad (26)$$

⁵Similarly, it can be shown that there are no corners between $(0, y_1)$ and (x_2, y_2) on any of the minimizing curves to be treated here.

From the relations of equation (26) it is clear, again, that the minimizing curve cannot pass through (0,0), the condition $y_1' = 1$ determining a value $y_1 > 0$. These relations, together with the volume condition (equation (7)) and the given length condition, serve to determine y_1 and λ and thus, of course, the shape of the entire body. As the length approaches 0, λ becomes infinitely negative; while, as the length becomes infinitely large, λ approaches 0. (In the latter case the body shape approaches the minimum-drag shape for the given length and diameter condition, $l/d \rightarrow \infty$.) Intermediate negative values of λ correspond to intermediate values of length for a given volume.

Given length and surface area.— In this case a first integral to the Euler equation is given by equation (18), and the parametric representation of the minimizing curve may be written immediately in the form

$$\left. \begin{aligned} y &= \frac{\text{const. } (1+y'^2)^2}{4y'^3 - \lambda(1+y'^2)^{3/2}} \\ x &= \int_{y_1}^y \frac{dy}{y'} \end{aligned} \right\} \quad (27)$$

Upon examination of this equation and equations (20) and (22), it becomes apparent that, again, the minimizing curve cannot go through the point (0,0). The latter equations determine uniquely, however, the values of y_1' ($y_1' < 1$), and y_2' ($0 < y_2' < y_1'$), in terms of the parameter λ . Similarly, the length and surface-area condition in combination with the above equations determines the value of λ . Thus it is easily shown that the practical range of λ is from -2 to 0 (corresponding to body lengths of from zero to infinity for a given surface area — in the latter case the Newton body is again obtained).

Given base diameter and volume.— With these given conditions, the first integral to the Euler relation is given by equation (17), while the terminal conditions at the fore-and-aft ends of the body are fixed by equations (19) and (21), respectively. It is evident that the minimizing curve must, in general, pass through the origin in order to satisfy all these equations in addition to the Legendre condition (equation (24)). The shape of the minimizing curve may thus be defined parametrically as follows:

$$\left. \begin{aligned} y &= \frac{4}{\lambda} \frac{y'^3}{(1+y'^2)^2} \\ x &= \frac{2}{\lambda} \frac{y'^4 + 3y'^2}{(1+y'^2)^2} \end{aligned} \right\} \quad (28)$$

where $y_1' = 0$. Combining this expression with equation (7), there is then obtained for the volume of the body

$$V = \frac{\pi y_2^3}{120 y_2'} (y_2'^4 + 6y_2'^2 + 45) \quad (29)$$

The range of λ for which these results are applicable⁶ is from zero to $3\sqrt{3}/4y_2$, corresponding to a volume range from infinity to $\pi y_2^3 \sqrt{3}/5$. For a given y_2 and a given $V > \pi y_2^3 \sqrt{3}/5$ (corresponding to $\frac{l}{d} > \sqrt{3}/2$), equation (29) has two solutions in y_2' . One solution yields values of y_2' greater than $\sqrt{3}$, which result violates the Legendre condition (see equation (24)), while the other yields permissible values less than $\sqrt{3}$. When y_2 and y_2' are known, λ may then be determined from the first relation of equation (28), namely,

$$\lambda = \frac{4}{y_2} \frac{y_2'^3}{(1+y_2'^2)^2} \quad (30)$$

The determination of y and x follows directly, of course, from equation (28).

Given base diameter and surface area.— In this case equations (18), (20), and (21) determine the shape of the minimizing curve as being simply a straight line

$$y = x \sqrt{\frac{(\lambda/4)^{2/3}}{1 - (\lambda/4)^{2/3}}} \quad (31)$$

where the parameter λ is given by the equation

⁶The solution given here is not applicable to bodies of extremely small fineness ratios (viz., $\frac{l}{d} < \frac{\sqrt{3}}{2}$) as can be easily deduced from equation (28).

$$\lambda = 4 (\pi y_2^2 / S)^3 \quad (32)$$

Thus, the minimum-drag body for given base diameter and surface area is a cone.

Comparison of Minimum-Drag Body Shapes

The previous calculation of minimum-drag bodies reveals two general characteristics of their shapes; namely, when the length is given (fixed) the bodies assume blunt noses, whereas, when the length is not given (i.e., is free), the bodies assume sharp noses. The former characteristic may be traced to the fact that with the length restricted, the net drag is reduced by accepting higher pressures on a relatively small area of large slope near the nose, thus achieving lower pressures on a relatively large area of small slope near the base. On the other hand, when the length is not restricted it is evident that a sharp rather than a blunt nose will obtain for minimum drag, since the drag of any blunt-nosed body can be reduced by simply relaxing the requirement on length, thereby allowing the body to be made sharp nosed and generally more slender.

In order to permit a quantitative comparison of the shapes of the calculated minimum-drag bodies, typical meridian curves for these bodies are shown in figure 2. For simplicity the bodies are compared on the basis of the same fineness ratio — ordinates have been plotted to an expanded scale to better indicate the relative shapes. The maximum bluntness is evidently obtained when the drag is minimized for a given length and surface area, while the maximum sharpness (a cusp nose) is obtained when the base diameter and volume are given. It is apparent from figure 2 that the flat-nosed portions of the meridian curves for the given length bodies are in all cases very small. For example, y_1 equals $0.0050y_2$ for the body of given length and volume. On the basis of several calculations it is indicated, as might be expected, that the degree of bluntness will increase with decreasing fineness ratio.

It is also of interest to compare minimum-drag body shapes determined with the aid of the linear theory (see, e.g., reference 2) with those found using the impact theory, that is, bodies especially suited for flight at low and high supersonic speeds, respectively. Such a comparison is shown in figure 3 for the case of given length and base diameter. It is seen that qualitatively the shapes are similar although the minimum-drag body for low supersonic speeds is generally the fatter

of the two.⁷ Comparisons of the results of this paper with those of reference 2 for other given conditions also indicate qualitative agreement as to general body shapes despite the marked difference in the laws governing the surface pressures.

All the preceding analysis has been predicated on the assumption that the flow of air at high supersonic speeds may, insofar as pressure forces are concerned, be approximated by a Newtonian-type flow. It remains now to test the accuracy of this assumption and other aspects of the analysis by experiment.

EXPERIMENT

It has been undertaken to obtain a partial check on the findings of the preceding theoretical analysis by determining experimentally the fore-drags on a family of bodies of given fineness ratios at Mach numbers from 2.73 to 6.28. The analysis may be expected to apply, at least approximately, in this range since for the bodies tested the corresponding values of the hypersonic similarity parameter K were, for the most part, greater than 1. A brief description of these tests is now presented.

Apparatus and Tests

The tests were conducted in the Ames 10- by 14-inch supersonic wind tunnel, which is of the continuous-flow nonreturn type and operates with a nominal supply pressure of 6 atmospheres. The Mach number in the test section may be varied from approximately 2.7 to 6.3 by changing the relative positions of the symmetrical top and bottom walls of the wind tunnel. During operation at the higher Mach numbers, the supply air is heated before it enters the wind tunnel to prevent condensation of the air. A detailed description of the wind tunnel and its associated equipment and of the characteristics of the flow in the test section may be found in reference 17.

Aerodynamic drag forces were measured with a strain-gage balance. Tare forces on the sting supports were essentially eliminated by shrouds that extended to within 0.040 inch of the model base. Axial forces on the bases of the models were determined from measured base pressures and from

⁷Part of this difference in shapes stems from the fact that the body derived using linear theory was required to have zero slope at the base. Also, as will be shown later, the true minimum-drag shape at high supersonic airspeeds may be somewhat fatter than that obtained using impact theory, due to the fact that centrifugal forces are neglected in this theory.

free-stream static pressures and were subtracted from measured total drag forces; thus, the data presented do not include the forces acting on the bases of the test bodies.

Reynolds numbers based on the maximum diameter of the test bodies were:

Mach number	Reynolds number, million
2.75	0.70
3.50	.95
4.00	.72
5.05	.35
6.28	.15

Reynolds numbers based on model length may be obtained by multiplying the above values by model fineness ratio.

Models

Five models of fineness ratio 3, and three models of fineness ratio 5 were tested. With the exception of an $l/d = 3$ tangent ogive (this shape was included as being typical of those in common usage), all models had meridian section shapes given by the equation

$$\frac{y}{d/2} = \left(\frac{x}{l}\right)^n \quad (33)$$

where n was given values of 1, $3/4$, $1/2$, and $1/4$. When $n = 3/4$, the body shapes defined by the above expression closely approximate the minimum-drag shapes for given length and base diameter (equation (25))⁸ for $l/d = 3$ and 5 (see fig. 4).

When $n = 1$, the cone is, of course, obtained which is the minimum-drag body for a given base diameter and surface area. Minimum-drag shapes for two different given conditions are thus included among the bodies tested.

Photographs of the eight models tested are shown in figure 5. The $l/d = 3$ bodies (fig. 5(a)) are, from left to right in the photograph, the cone, $3/4$ -power body, $1/2$ -power (parabolic) body, $1/4$ -power body, and the tangent ogive which has a profile section radius of curvature of 9.25 body diameters. From left to right in figure 5(b) are the $l/d = 5$ cone, $3/4$ -power body, and $1/2$ -power body. The base diameter of all models was 1 inch.

⁸The accuracy of this approximation increases with increasing values of l/d as can easily be seen upon examination of equation (25).

Accuracy of Test Results

The accuracy of the foredrag coefficients is effected by uncertainties in the measurements of the following quantities: stagnation pressures, free-stream static pressures, base pressures, and the forces on the models as measured by the strain-gage balance.

Both static and free-stream dynamic pressures were determined from wind-tunnel calibration data and stagnation-pressure readings. The latter measurements were accurate to within $\pm 1/2$ percent, thus static and dynamic pressures are uncertain by this amount plus possible calibration errors of ± 1 percent over the Mach number range of the tests. The uncertainty in foredrags due to inaccuracies in the determination of base pressures does not exceed ± 1 percent.

Because of the small drag forces measured, the source of greatest error was the strain-gage balance system. The uncertainty in drag due to zero shifts, thermal effects, and friction varied from approximately ± 2 percent at the lower Mach numbers to ± 6 percent at the highest Mach numbers.

The combined effects of all the sources of error result in probable uncertainties in measured foredrag coefficients of from ± 0.001 at the low Mach numbers to ± 0.005 at a Mach number of 6.28. In order to reduce this error in the data presented here, particularly at the higher Mach numbers, several measurements were made at each Mach number and the average values of foredrag coefficients were employed.

RESULTS AND DISCUSSION

The variations with Mach number of the measured foredrag coefficients are shown in figure 6. It is evident that the $3/4$ -power bodies do, as predicted, have the minimum foredrags of all the test bodies with the same fineness ratio, the drag of the $3/4$ -power body being as much as 20 percent less than that of the cone of the same fineness ratio. The general increase in foredrag at Mach numbers in the neighborhood of 5 and greater can be traced to an increase in friction drag. This latter increase is, in turn, caused by the relatively large decrease in Reynolds number with increasing Mach number in this range (see section on Apparatus and Tests).

A check on the over-all accuracy with which the optimum shapes are predicted by the analysis is obtained by comparing theoretical and experimental values of the relative foredrag coefficients of the test bodies. Such a comparison is given in figure 7 where the ratios of the foredrag coefficients of a test body to the corresponding coefficients of the cone of the same fineness ratio are shown as a function of the exponent n in equation (33) which defines the shapes of the test bodies. The theoretical predictions of the impact theory appear to be in good agreement with the experimental results at the higher values of n (approximately $n > 0.6$). Thus it is suggested that the $3/4$ -power body is a reasonable approximation

to the correct minimum-foredrag shape of given fineness ratio. At the lower values of n , however, it is indicated that the relative drag is significantly overestimated by this theory. This result is not entirely surprising since the theory neglects centrifugal-force effects in the disturbed flow, and these effects must appreciably alter the pressures over the highly curved noses of the blunter bodies.

As discussed earlier, the Busemann theory for infinitely high Mach numbers overestimates these effects at the Mach numbers of interest here. It has therefore been undertaken in Appendix A of this paper to obtain a better estimate of centrifugal forces by accounting approximately for the decrease in these forces (at finite but high Mach numbers) associated with the increase in the lateral extent of the disturbed flow field with increasing distance downstream from the nose of the body. The predictions of the modified impact theory shown in figure 7 were obtained with the aid of this estimated centrifugal-force effect (see equation (A9)) in combination with equations (1) and (3). It is indicated that this theory is markedly superior to the impact theory at the lower values of n , corresponding to the blunter bodies, over the test Mach number range. The estimate of the centrifugal forces would thus appear to be in fair agreement with the actual magnitude of these forces.

It is also indicated in figure 7 that at the higher test Mach numbers (hence higher values of K),⁹ the modified theory is generally somewhat superior to the impact theory. This result suggests that improved approximations to the correct minimum-foredrag shapes for values of K appreciably greater than 1 may be obtained by using this theory rather than the simple impact theory. Accordingly, calculations of minimum-drag shapes have been made using the modified impact theory in the manner discussed in Appendix B. The body shapes obtained (see Appendix B) are for the same given geometric conditions as those previously determined using impact theory. The resulting shape for given length and diameter is shown in figure 8. Newton's body of the same fineness ratio is also shown for comparison. The body shape determined by the modified theory is somewhat more blunt in the region of the nose and has more curvature in the region downstream of the nose than Newton's body. A similar comparison is shown in figure 9 for the bodies of given base diameter and surface area. In this case both bodies have pointed noses because the length is not fixed, but, in the same manner as for the bodies of given fineness ratio, the shape calculated with the modified theory has more curvature in the region aft of the nose than does the body calculated with the impact theory. This result is not surprising in view of the pressure relieving effect of centrifugal forces.

Calculation of the drag of these bodies indicates that those obtained using Newtonian theory will as expected have the higher drag at hypersonic speeds, although not by more than a few percent. This result suggests

⁹The highest value of K in the present tests was 2.1.

that consideration of centrifugal forces will, in the practical case, principally influence the shape and not the drag of minimum drag bodies.

CONCLUDING REMARKS

It has been undertaken in this report to determine approximately the shapes of several bodies having minimum pressure foredrag at high supersonic airspeeds. With the aid of Newton's law of resistance and the calculus of variations, an investigation was carried out for various combinations of the conditions of given body length, base diameter, surface area, and volume. In general, it was found that when the length is fixed, the body has a blunt nose (i.e., a finite area of infinite slope at the nose) as in the classical problem considered by Newton; whereas when the length is not fixed the body has a sharp nose.

Several bodies of revolution of fineness ratios 3 and 5, including the calculated minimum-drag bodies for given length and base diameter and for given base diameter and surface area, were tested at Mach numbers from 2.73 to 6.28 in the Ames 10- by 14-inch supersonic wind tunnel. A comparison of the relative theoretical and experimental foredrag coefficients indicated that the calculated minimum-drag bodies were reasonable approximations to the correct shapes. It was verified, for example, that the minimum-drag body for a given length and base diameter has as much as 20 percent less foredrag than a cone of the same fineness ratio. The cone is, however, the calculated minimum-drag body for a given base diameter and surface area.

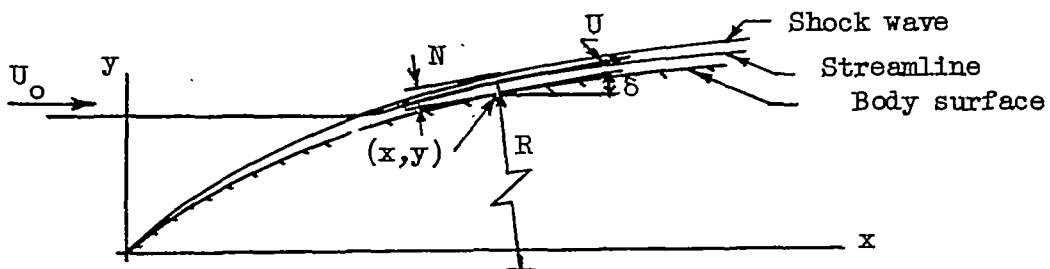
The comparison between theory and experiment also indicated that the centrifugal forces in the flow about bodies curved in the stream direction may influence their drag. The relative extent of this influence was found to be predictable, particularly at the higher Mach numbers, with a simple modification to the impact theory of Newton. It was therefore suggested that improved approximations to minimum foredrag shapes at high supersonic airspeeds (for which the hypersonic similarity parameter has a value appreciably greater than 1) may be calculated with the aid of the modified impact theory. Such a calculation was carried out for bodies with the same given conditions as those calculated with the Newtonian theory. In general, the resulting shapes were found to be somewhat blunter in the region of the nose, to have more curvature in the region downstream of the nose, and to have slightly lower drag than the corresponding shapes obtained using the simple impact theory.

Ames Aeronautical Laboratory
National Advisory Committee for Aeronautics
Moffett Field, Calif., Dec. 14, 1955

APPENDIX A
ESTIMATED EFFECT OF CENTRIFUGAL FORCES
ON SURFACE PRESSURE COEFFICIENTS

An estimate of the effect of centrifugal forces on the pressures at the surface of a body operating at high but finite Mach numbers may be obtained by comparing the disturbance flow fields at these Mach numbers with that associated with infinitely large Mach number.

At high Mach numbers the disturbed air flows in a relatively thin region (sometimes termed the hypersonic boundary layer) between the bow shock wave and the surface of the body (see sketch).



The change in pressure from the surface to the shock due to centrifugal forces in the fluid is given by the equation

$$\Delta p = \int_0^N \frac{dp}{dN} dN = \int_0^N \frac{\rho U^2}{R} dN$$

assuming the directions of the normals to the streamlines between the surface and the shock do not differ appreciably from the direction of the normal to the surface. This expression is more conveniently written in the form

$$\Delta p = \frac{\bar{U}}{R} \int_0^N \rho UdN \quad (A1)$$

where \bar{U} and \bar{R} are mean values of the velocity and radius, respectively, in the interval N . Now the mass m of air between the surface and the shock flowing (in unit time) by a point on the body is given by the relation

$$m \cong 2\pi y \int_0^N \rho UdN \cong \pi y^2 \rho_0 U_0 \quad (A2)$$

Combining equations (A1) and (A2) there is then obtained for the pressure change

$$\Delta p = \frac{\bar{U}}{R} \frac{y}{2} \rho_0 U_0$$

or in coefficient form

$$\Delta C_p = \frac{\Delta p}{q_0} = \frac{y}{R} \frac{\bar{U}}{U_0} \quad (A3)$$

Now in the limit as the Mach number approaches infinity and γ of the disturbed fluid approaches 1, the thickness of the layer becomes infinitesimal and hence

$$\bar{R} = R_B \quad (A4)$$

Similarly, it is easily shown (e.g., with the compatibility equations applying along characteristic lines in axially symmetric supersonic flow) that

$$dU = 0$$

along any streamline downstream of the bow shock, and thus that

$$\bar{U} = \frac{2U_0}{y^2} \int_0^y y \cos \delta dy \quad (A5)$$

Hence, in this limiting case, equation (A3) takes on a form equivalent to that first deduced by Busemann (see second term on right of equation (2)), and later derived in reference 18, namely,

$$\Delta C_p = \frac{2}{R_B y} \int_0^y y \cos \delta dy \quad (A6)$$

where

$$\frac{1}{R_B} = \sin \delta \frac{d\delta}{dy}$$

On the other hand when the Mach number is finite, but high, and γ of the disturbed fluid is closer to 1.4 than 1, the preceding evaluations of \bar{R} and \bar{U} are in considerable error since the hypersonic boundary layer, although thin, is no longer of infinitesimal thickness. This change in the boundary layer results from the fact that the bow shock is detached (except perhaps at the nose) from the surface of the

body, the lateral distance from the surface to the shock increasing with increasing distance downstream from the nose (see sketch). Thus, for example, \bar{R} would be expected to approach R_B only near the nose, while with increasing distance downstream of the nose it would be expected to become larger than R_B . From the pressure distributions presented in reference 13 it is indicated, in fact, that for $K > 1$ (the range of K 's of interest in this paper) $\bar{R} > R_B$ near the maximum ordinate of the body. (This indication follows from the small values of the pressure coefficients near the maximum ordinate.) It is suggested, therefore, that at the high supersonic speeds under consideration, an approximation to \bar{R} is given by the relation

$$\frac{\bar{R}}{R_B} = \frac{1}{1 - \frac{y}{y_2}} \quad (A7)$$

Similarly, in the case of \bar{U} it no longer follows that the magnitude of the velocity must be constant along streamlines downstream of the bow shock since pressure disturbances can now be transmitted across streamlines. Thus a better first approximation to \bar{U} than that given by equation (A5) may be obtained from the simple corpuscular or impact theory,¹⁰ namely,

$$\bar{U} = U_0 \cos \delta \quad (A8)$$

Combining equations (A3), (A7), and (A8), the estimated change in pressure coefficient at the surface of a body due to centrifugal forces in high supersonic speed flow is obtained in the form

$$\Delta C_p = \frac{Y}{R_B} \left(1 - \frac{Y}{y_2}\right) \cos \delta$$

or

$$\Delta C_p = \frac{Y}{2} \left(1 - \frac{Y}{y_2}\right) \frac{d}{dy} (\sin^2 \delta) \quad (A9)$$

¹⁰With this theory, acceleration of the flow along a streamline is qualitatively accounted for.

APPENDIX B

CALCULATION OF MINIMUM-DRAG BODIES, WITH
 CONSIDERATION OF CENTRIFUGAL FORCES
 IN THE DISTURBED FLOW FIELD

Given Length and Base Diameter

For the purpose of this calculation, equations (1) and (A9) for the pressure coefficient are combined with equation (4) to yield the drag parameter in the form

$$I_D = y_1^2 + \varphi(y_1) + \int_0^{x_2} \left[2 \sin^2 \delta + \frac{y}{2} \left(1 - \frac{y}{y_2}\right) \frac{d}{dy} \sin^2 \delta \right] yy' dx \quad (B1)$$

The term y_1^2 represents the drag on any finite region of infinite slope at the nose, while the function $\varphi(y_1)$, given by¹¹

$$\varphi(y_1) = -\frac{y_1^2}{2} \left(1 - \frac{y_1}{y_2}\right) \cos^2 \delta_1$$

represents a "leading-edge thrust" due to the acceleration of the air flow about a corner (if it exists) at $(0, y_1)$.

The expression (B1) may be put in the form

$$I_D = y_1^2 + \int_0^{x_2} \left\{ \left[2 \sin^2 \delta + \frac{y}{2} \left(1 - \frac{y}{y_2}\right) \frac{d}{dy} \sin^2 \delta \right] yy' - \frac{d}{dx} \varphi(y) \right\} dx$$

whereupon (recalling $\sin^2 \delta = \frac{y'^2}{1+y'^2}$) the integrand simplifies to a function f given by the relation

¹¹This function may be obtained by evaluating

$$\lim_{\epsilon \rightarrow 0} \int_{y_1-\epsilon}^{y_1+\epsilon} \frac{y^2}{2} \left(1 - \frac{y}{y_2}\right) \frac{d}{dy} (\sin^2 \delta) dy$$

along the body-surface streamline about the corner at $(0, y_1)$.

$$f = yy^* \left(2 - \frac{1 + \frac{3}{2} \frac{y}{y_2}}{1 + y^{*2}} \right)$$

With the aid of this expression and equations (15) and (19) the parametric representation of the minimizing curve can be obtained in the following form:

$$\left. \begin{aligned} y &= \frac{y_2}{3} \left[-1 + \sqrt{1 + \frac{15y_2^{*3}}{(1 + y_2^{*2})^2} \frac{(1 + y^{*2})^2}{y^{*3}}} \right] \\ x &= \int_{y_1}^y \frac{dy}{y^*} \end{aligned} \right\} \quad (B2)$$

where

$$y_1^* = 1$$

and, in general,

$$y_1 > 0$$

The minimizing curve given by these relations, similar to the curve obtained from the impact pressure treatment, does not have a corner between the points $(0, y_1)$ and (x_2, y_2) . The minimum-drag shape defined by equation (B2) is compared in figure 8 with that determined earlier by considering impact pressures only.

The equations defining the minimizing curves for the other given geometric conditions are obtained in a similar manner.

Given Length and Volume

$$\left. \begin{aligned} y &= \frac{-y^{*3} + \sqrt{y^{*6} + c(1 + y^{*2})^2 \left[\frac{3y^{*3}}{y_2} - \lambda(1 + y^{*2})^2 \right]}}{\frac{3y^{*3}}{y_2} - \lambda(1 + y^{*2})^2} \\ x &= \int_{y_1}^y \frac{dy}{y^*} \end{aligned} \right\} \quad (B3)$$

with $y_1' = 1$ and $y_2' = 0.274$ and a range of λ from $-\infty$ to 0 corresponding to the range 0 to ∞ for l .

Numerical integration of equation (B3) is accomplished by first evaluating the first integral to the Euler equation at the base of the body and solving for c/y_2 in terms of $y_2\lambda$. Letting $\phi(y', y_2\lambda)$ represent the resulting function of y' and $y_2\lambda$, equation (B3) becomes

$$y = y_2\phi(y', y_2\lambda)$$

$$l = \int_{y_1'}^{y_2} \frac{dy}{y'} = y_2 \int_{y' = 1}^{0.274} \frac{d\phi}{y'} = y_2 \Lambda(y_2\lambda)$$

and the volume is given by

$$\frac{V}{\pi} = y_2^3 \int_{y' = 1}^{0.274} \phi^2 \frac{d\phi}{y'} = y_2^3 \Gamma(y_2\lambda)$$

The values of the functions Λ and Γ are obtained by numerical integration for various values of $y_2\lambda$ to enable interpolation for that value of $y_2\lambda$ which makes $\Gamma/\Lambda^3 = V/\pi l^3$. The set $(y_2\lambda, \Lambda, \Gamma)$ so determined satisfies the given volume and length requirements and yields a value of the base ordinate, $y_2 = l/\Lambda$.

Given Length and Surface Area

$$y = \frac{1}{6y'^3} \left\{ \left[\lambda(1 + y'^2)^{3/2} - 2y'^3 \right] y_2 \pm \sqrt{\left[\lambda(1 + y'^2)^{3/2} - 2y'^3 \right]^2 y_2^2 + 12cy'^3(1 + y'^2)^2 y_2} \right\} \quad (B4)$$

$$x = \int_0^y \frac{dy}{y'}$$

with a range of λ given by

$$-0.64 < \lambda < 2 \left(1 + \frac{3y_1}{2y_2} \right)$$

The procedure used to integrate equations (B4) is similar to that employed to integrate equations (B3) above.

Given Base Diameter and Volume

$$\left. \begin{aligned} y &= \frac{2y_2}{\lambda y_2 (1 + y^2)^2 - 3} \\ x &= \int_{y_1}^y \frac{dy}{y^4} \end{aligned} \right\} \quad (B5)$$

where

$$\lambda y_2 = 5y_2^3 / (1 + y_2^2)^2$$

For l/d ratios greater than $1/2$, $y_1 = 0$, $y_1' = 0$, and the ranges of y_2' and λ are

$$0 \leq y_2' \leq \sqrt{3}$$

$$0 \leq \lambda \leq 3 \frac{\sqrt{3}}{16}$$

Given Base Diameter and Surface Area

$$\left. \begin{aligned} y &= \frac{y_2}{3} \left[\lambda \frac{(1 + y^2)^{3/2}}{y^4} - 2 \right] \\ x &= \int_{y_1}^y \frac{dy}{y^4} = \frac{\lambda y_2}{8} \left[\frac{2(1 + y^2)^{3/2}}{y^4} + \frac{\sqrt{1 + y^2}}{y^2} - l \eta \frac{1 + \sqrt{1 + y^2}}{y^4} - c \right] \end{aligned} \right\} \quad (B6)$$

with $y_1 = 0$ and

$$\lambda = 121.6(y_2^2/S)^3$$

The minimizing curve given by equations (B6) is compared in figure 9 with that determined earlier (the cone) by considering impact pressures only.

REFERENCES

1. von Kármán, Th.: The Problem of Resistance in Compressible Fluids. GALCIT Pub. No. 75, 1936. (From R. Acad. D'Italia, vol. XIV, Roma, 1936)
2. Haack, W.: Projectile Forms of Minimum Wave Resistance. (Translation) Douglas Aircraft Company, Inc., Rept. 288, 1946.
3. Ferrari, Carlo: The Determination of the Projectile of Minimum Wave Resistance. Reale Academia della Science de Torino Atti, 1939. (Issued as British, M.A.P. RTP Tr. 1180)
4. Lighthill, M. J.: Supersonic Flow Past Bodies of Revolution. R. & M. No. 2003, British A.R.C., 1945.
5. Sears, William R.: On Projectiles of Minimum Wave Drag. Quart. App. Math., vol. IV, no. 4, Jan. 1947, pp. 361-366.
6. Newton, Isaac: Principia - Motte's Translation Revised. Univ. of Calif. Press, 1946, pp. 333, 657-661.
7. Sanger, Eugene: Raketen-flugtechnik. R. Oldenbourg (Berlin), 1933, pp. 120-121.
8. Epstein, P. S.: On the Air Resistance of Projectiles. Proceedings of National Academy of Sciences, 1931, vol. 17, pp. 532-547.
9. Forsyth, A. R.: Calculus of Variations. The Cambridge Univ. Press (England), 1927, pp. 320-324.
10. Bethe, H. E., and Teller, E.: Deviations from Thermal Equilibrium in Shock Waves. Ballistic Research Laboratory Rep. No. X-117, Aberdeen Proving Ground, Aberdeen, Md., 1945.
11. Eggers, A. J., Jr.: One-Dimensional Flow of an Imperfect Diatomic Gas. NACA Rep. 959, 1950. (Formerly NACA TN 1861)
12. Busemann, A.: Flussigkeits-und Garbewegung. Handwörterbuch der Naturwissenschaften. Gustav Fischer, Zweite Auflage, Jena, 1933.
13. Rossow, Vernon J.: Applicability of Hypersonic Similarity Rule to Pressure Distributions Which Include the Effects of Rotation for Bodies of Revolution at Zero Angle of Attack. NACA 2399, 1951.

14. Eggers, A. J., Jr., and Savin, Raymond C.: Approximate Methods for Calculating the Flow About Nonlifting Bodies of Revolution at High Supersonic Airspeeds. NACA TN 2579, 1951.
15. Bolza, Oskar: Lectures on the Calculus of Variations. G. E. Stechert and Co., New York, 1946 (1904 edition), pp. 22, 27, 38, 40, and 47.
16. Courant, R., and Hilbert, D.: Methoden der Mathematische Physik. J. Springer (Berlin), vol. 1, 1929, pp. 179-180.
17. Eggers, A. J., Jr., and Nothwang, George J.: The Ames 10- by 14-Inch Supersonic Wind Tunnel. NACA TN 3095, 1954.
18. Ivey, H. Reese, Klunker, E. Bernard, and Bowen, Edward N.: A Method for Determining the Aerodynamic Characteristics of Two- and Three-Dimensional Shapes at Hypersonic Speeds. NACA TN 1613, 1948.

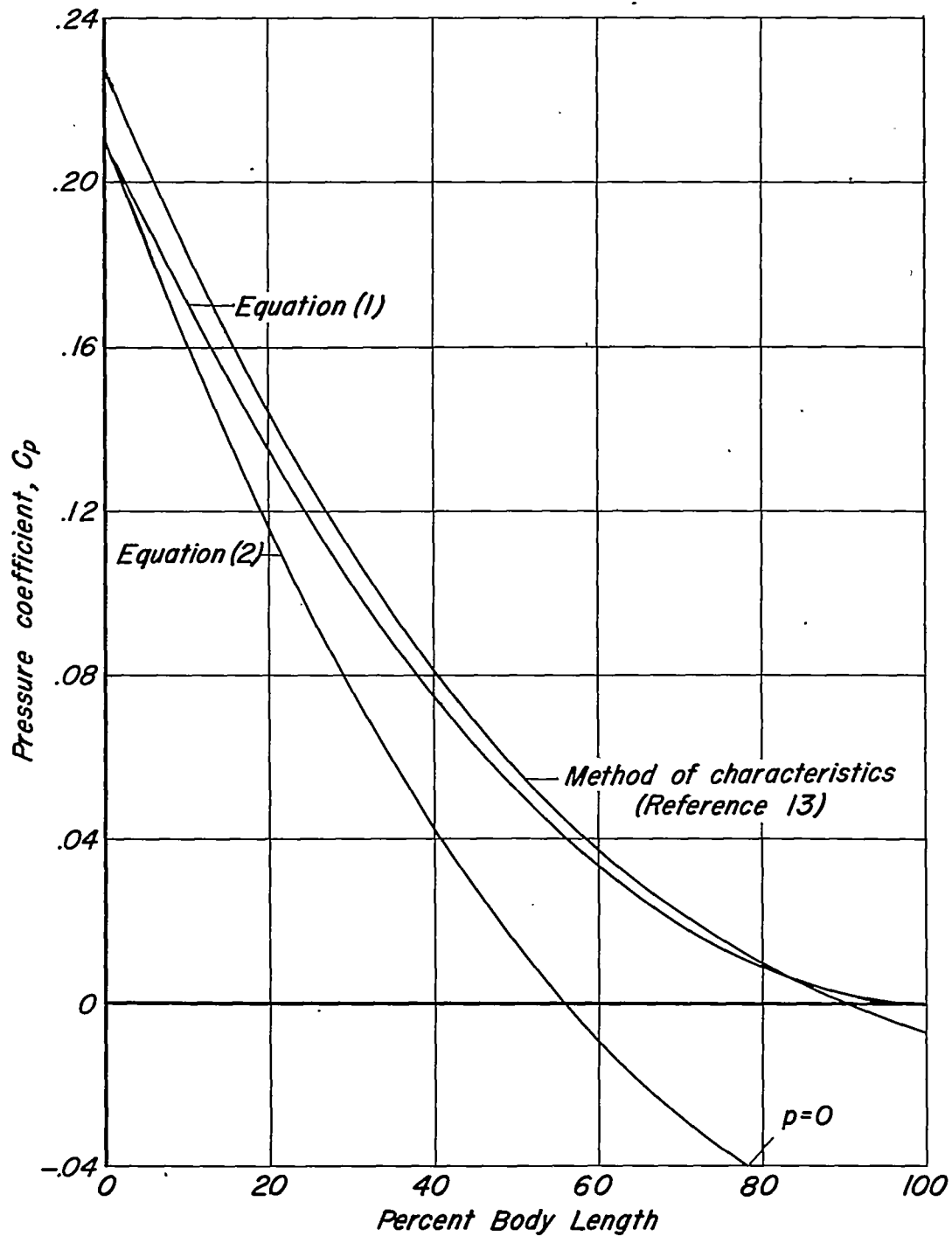


Figure 1.—Comparison of approximate and exact pressure distributions over a tangent ogive of fineness ratio 3 operating at a Mach number of 6 ($K=2$).

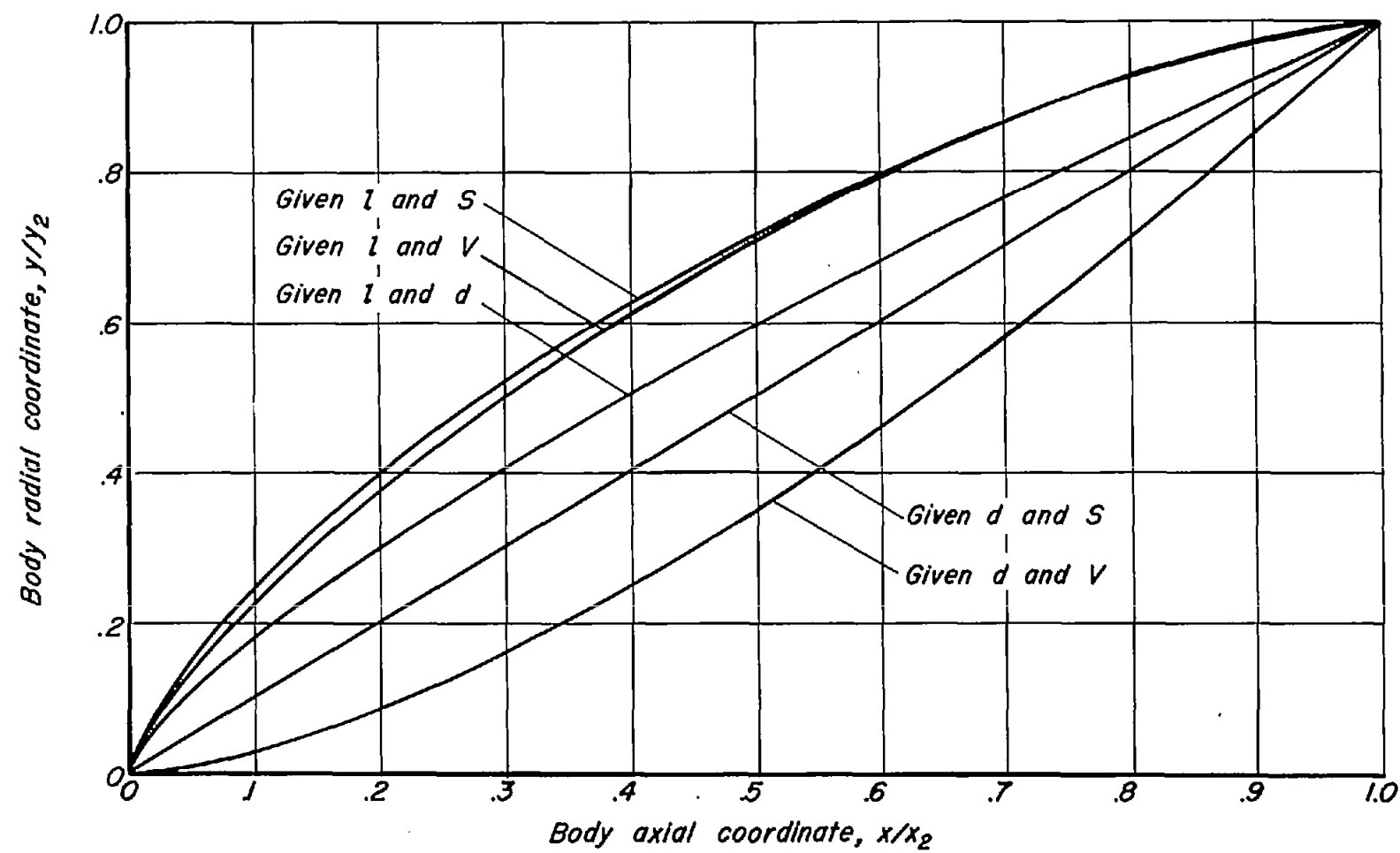


Figure 2.—Minimum drag bodies for various given conditions. ($l/d=5.0$ for all bodies)

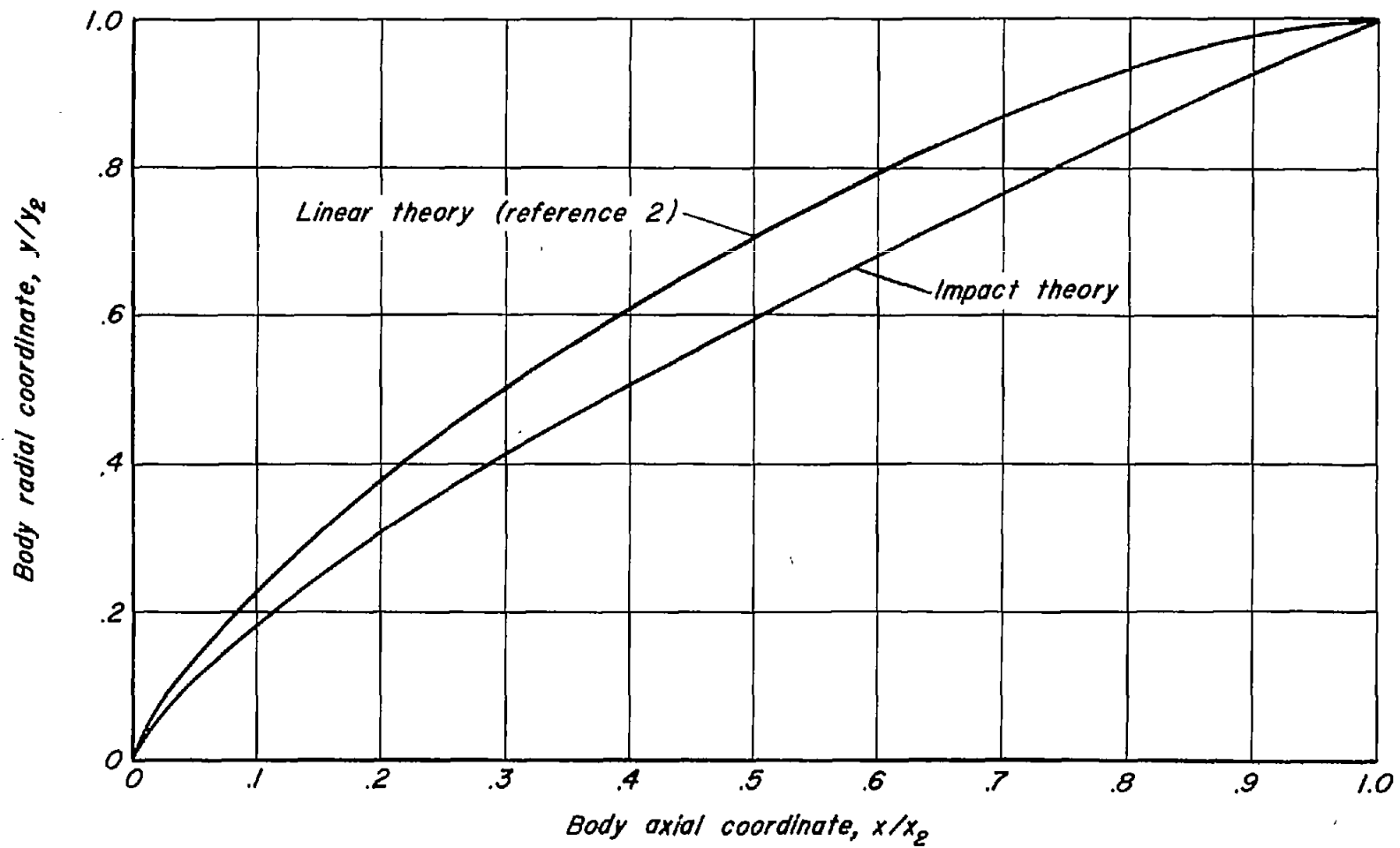


Figure 3.-Comparison of minimum drag bodies of given length and base diameter determined by linear theory and by impact theory.

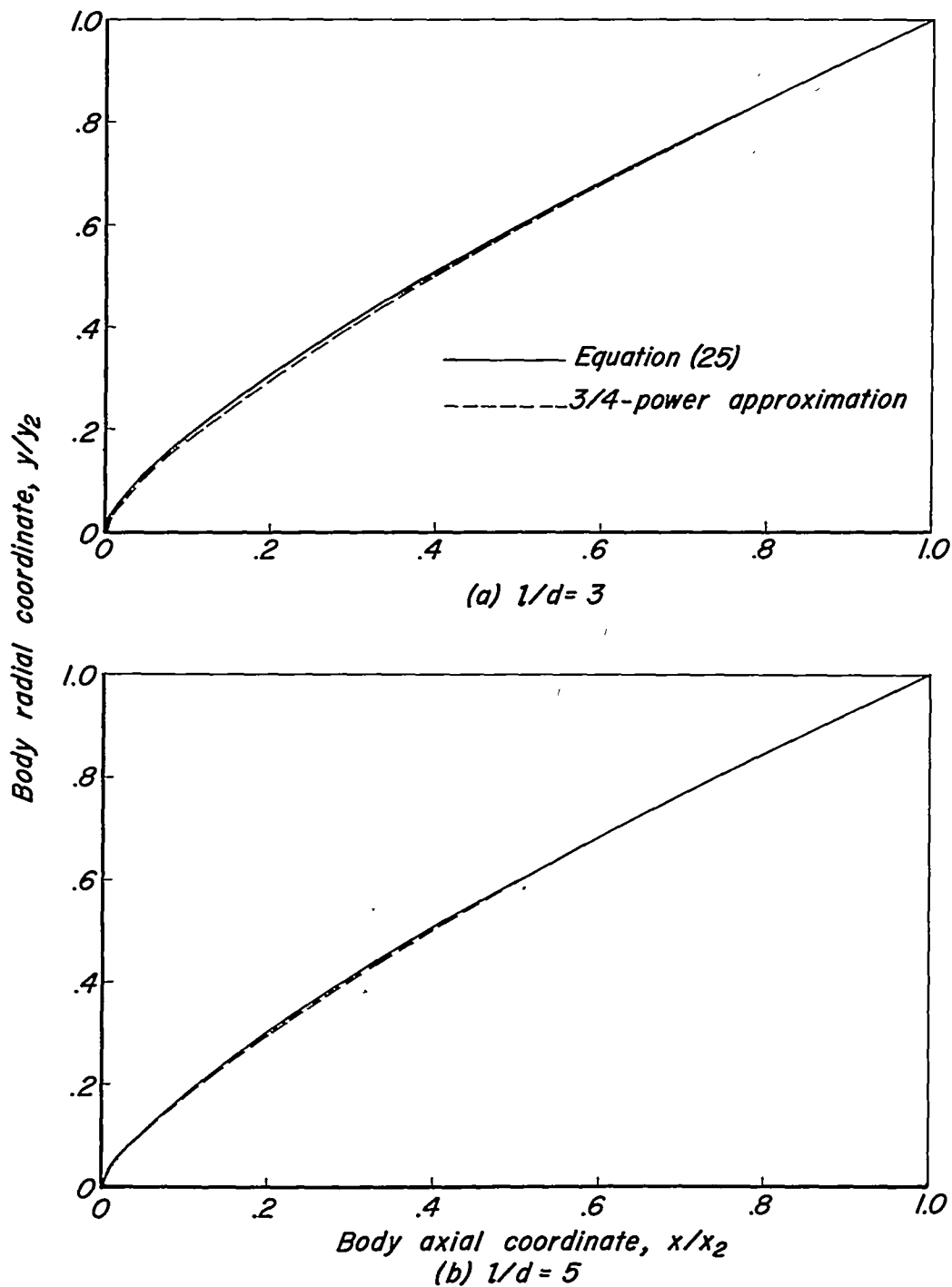
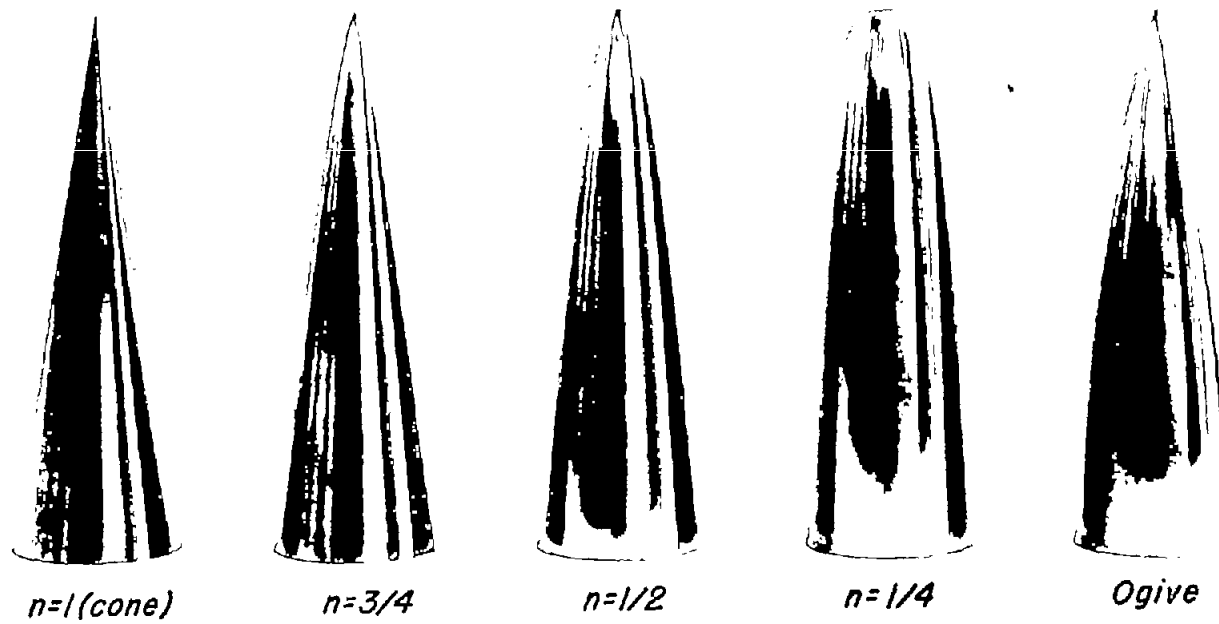


Figure 4.— Comparison of profiles of minimum drag bodies of revolution for given lengths and base diameters with the approximate profiles employed in the present tests.

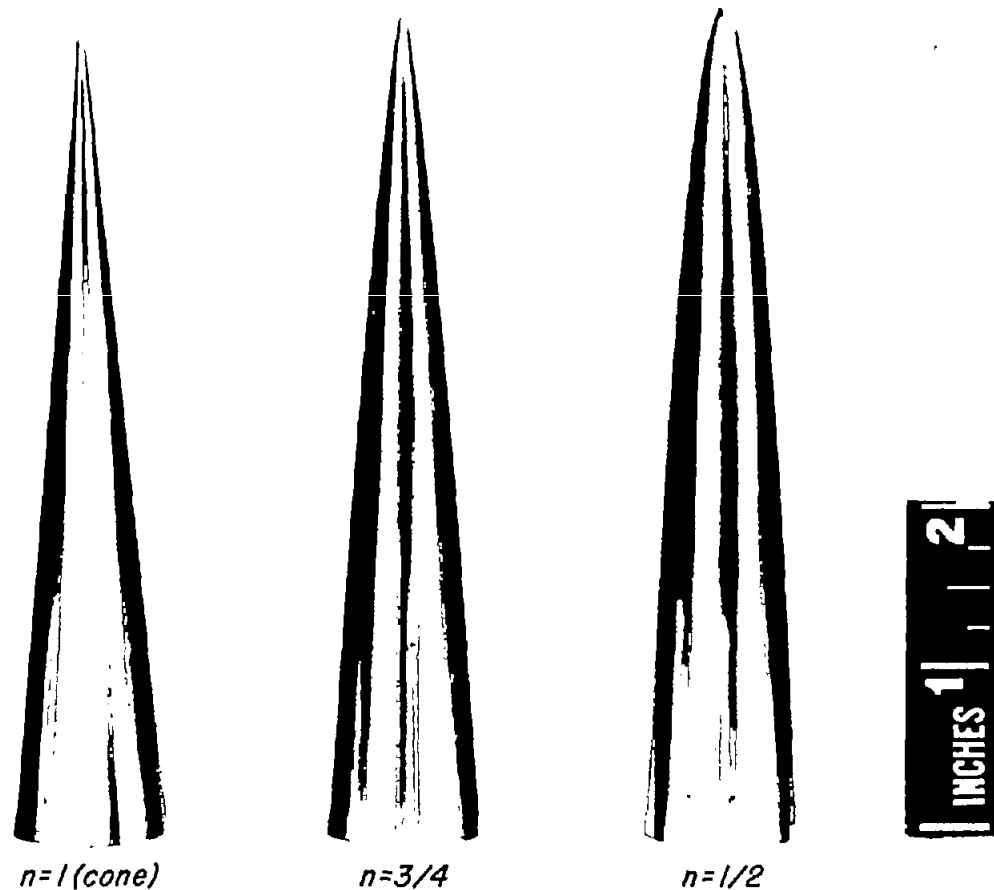


(a) Fineness ratio 3 bodies.

A-16674.1

Figure 5.-- Photographs of the seven test bodies, the shapes of which are given by the equation

$$y = \frac{d}{2} (x/l)^n, \text{ and the } l/d = 3 \text{ tangent ogive.}$$



(b) Fineness ratio 5 bodies.

Figure 5.- Concluded.

A-16236.2

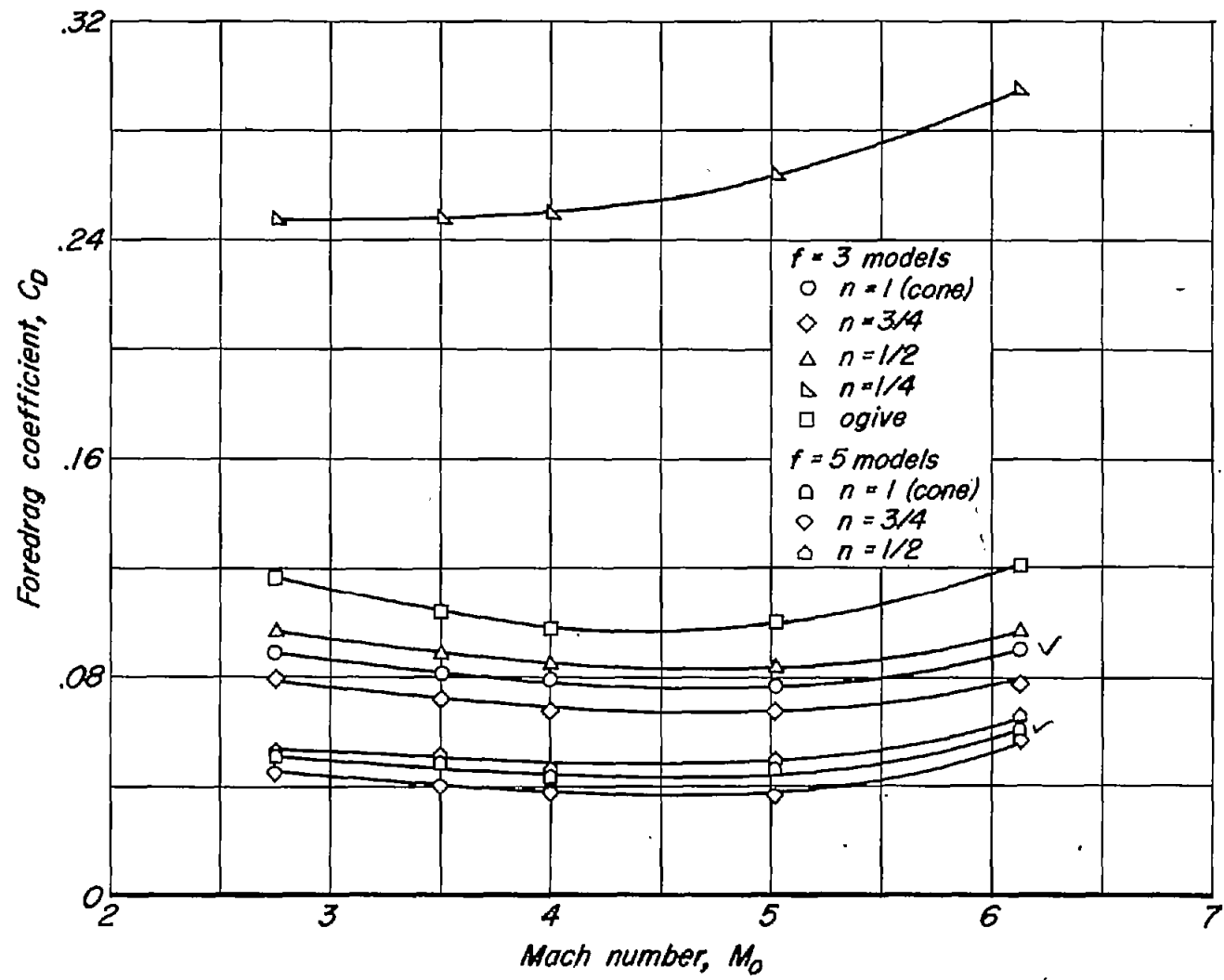


Figure 6.— The variation with Mach number of the foredrag coefficients at zero lift of the test bodies.

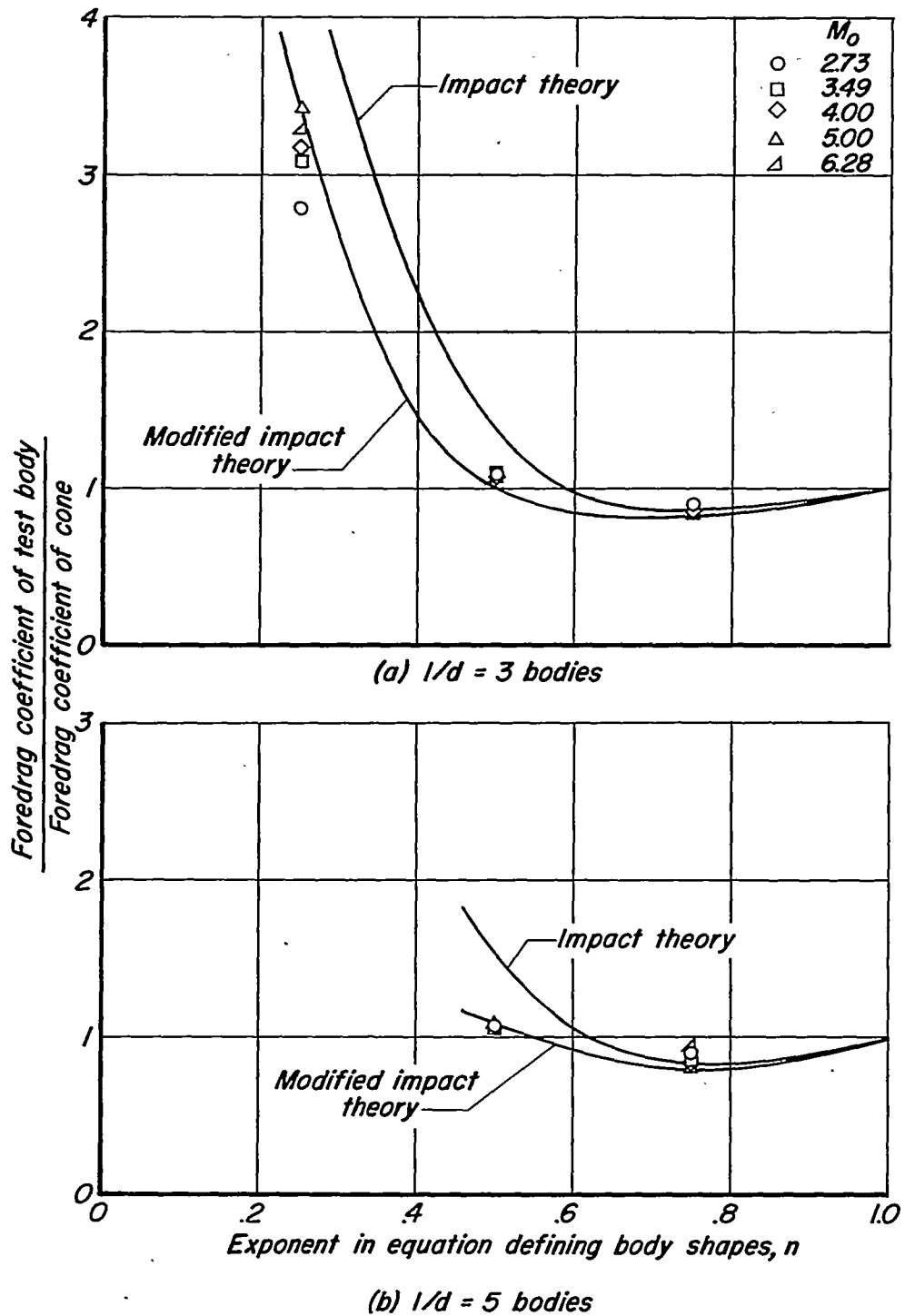


Figure 7.—The ratios of foredrag coefficients of test bodies to foredrag coefficients of cones as functions of the exponent, n , in the equation defining body shapes.

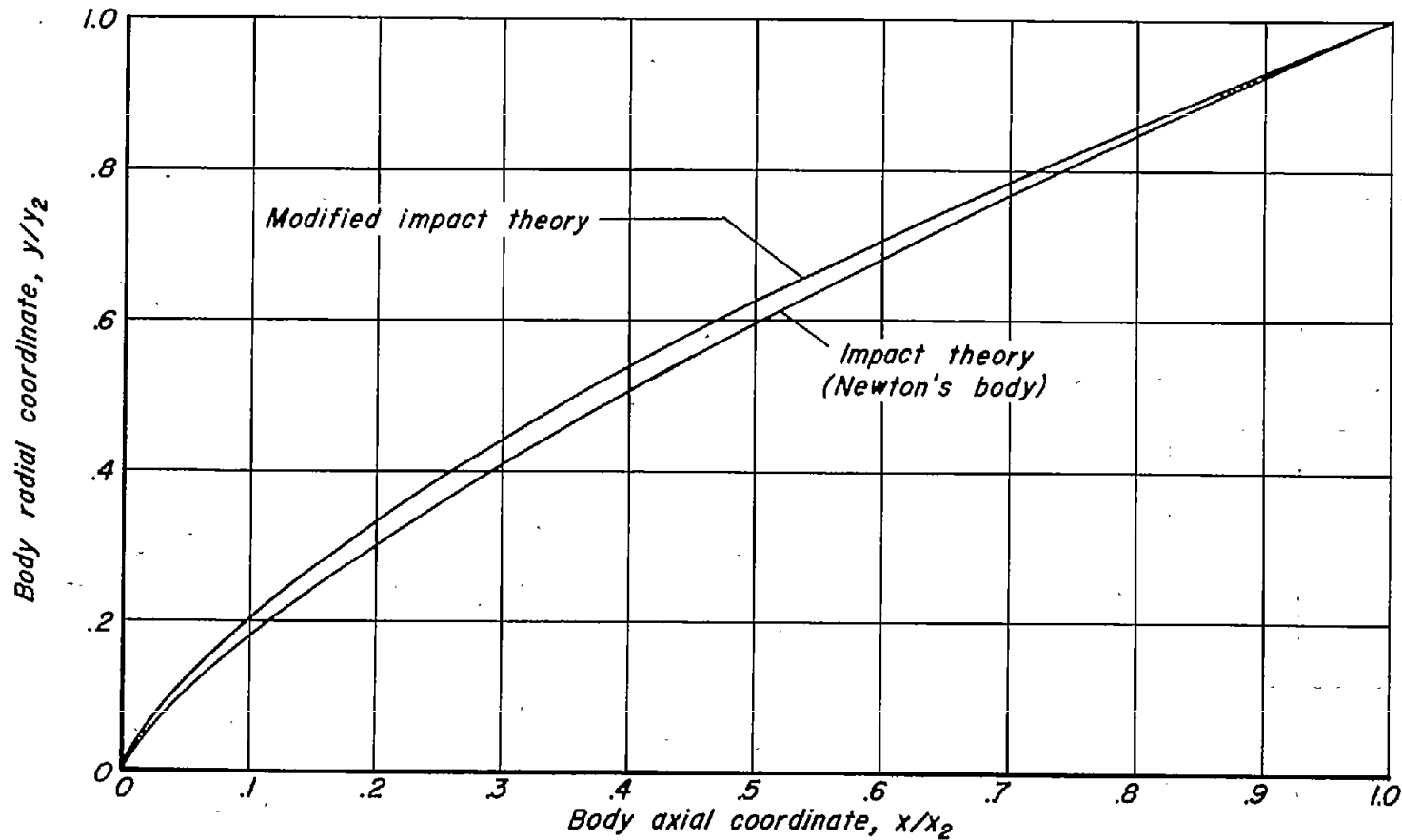


Figure 8.- The effect of centrifugal forces on the shape of the minimum drag body of given length and base diameter. ($V/d = 6.18$)

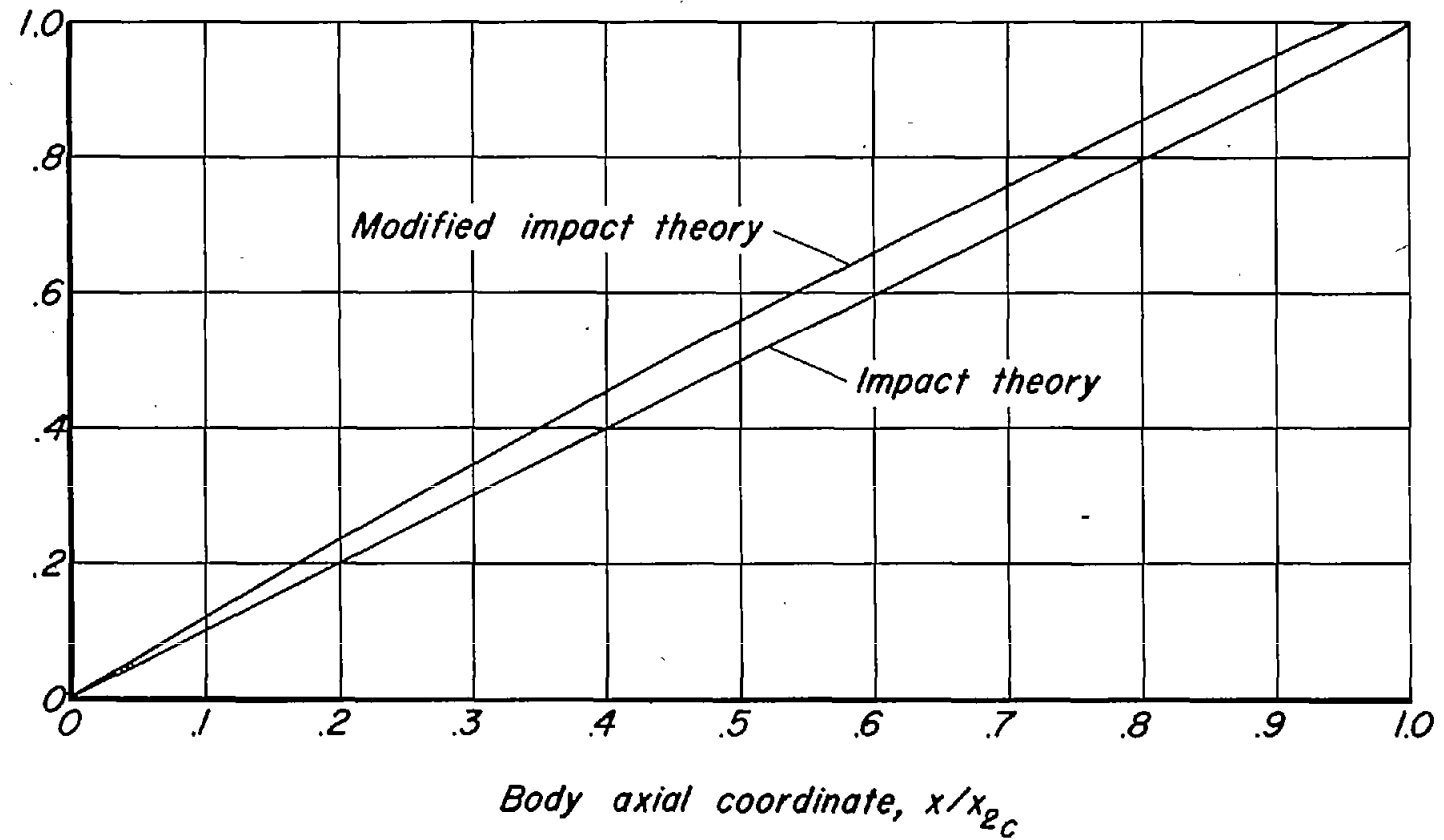


figure 9.- The effect of centrifugal forces on the shape of the minimum drag body of given diameter and surface area ($d = 2$, $S = 31.57$).